

Published in final edited form as:

Mol Cancer Ther. 2014 January ; 13(1): 60–70. doi:10.1158/1535-7163.MCT-13-0518.

Enhanced PI3K p110 α signaling confers acquired lapatinib resistance which can be effectively reversed by a p110 α -selective PI3K inhibitor

Samuel W Brady^{1,2}, Jian Zhang¹, Daniel Seok¹, Hai Wang¹, and Dihua Yu^{1,2}

¹Department of Molecular and Cellular Oncology, The University of Texas MD Anderson Cancer Center, Houston, Texas

²Cancer Biology Program, The University of Texas Health Science Center at Houston Graduate School of Biomedical Sciences, Houston, Texas.

Abstract

While the HER2-targeting agents trastuzumab and lapatinib have improved the survival of patients with HER2-positive breast cancer, resistance to these targeted therapies is a major challenge. To investigate mechanisms of acquired lapatinib resistance, we generated acquired lapatinib resistance cell models by extended exposure of two HER2-positive breast cancer cell lines to lapatinib. Genomic and proteomic analyses revealed that lapatinib-resistant breast cancer cells gained additional PI3K activation through activating mutation in PI3K p110 α and/or increasing protein expression of existing mutant p110 α . p110 α protein up-regulation in lapatinib-resistant cells occurred through gene amplification or post-transcriptional upregulation. Knockdown of p110 α , but not p110 β , the other PI3K catalytic subunit present in epithelial cells, inhibited proliferation of lapatinib-resistant cells, especially when combined with lapatinib. Lapatinib-resistant xenograft growth was inhibited persistently by combination treatment with the p110 α -selective PI3K inhibitor BYL719 and lapatinib; the drug combination was also well-tolerated in mice. Mechanistically, the combination of lapatinib plus BYL719 more effectively inhibited Akt phosphorylation and, surprisingly, Erk phosphorylation, than either drug alone in the resistance model. These findings indicate that lapatinib resistance can occur through p110 α protein upregulation-mediated, and/or mutation-induced, PI3K activation. Moreover, a combinatorial targeted therapy, lapatinib plus BYL719, effectively overcame lapatinib resistance in vivo and could be further tested in clinical trials. Finally, our findings indicate that p110 β may be dispensable for lapatinib resistance in some cases. This allows the usage of p110 α -specific PI3K inhibitors and thus may spare patients the toxicities of pan-PI3K inhibition to allow maximal dosage and efficacy.

Introduction

HER2 is a receptor tyrosine kinase (RTK) overexpressed in 25% of breast cancers (1). HER2 overexpression leads to ligand-independent receptor dimerization and phosphorylation, including phosphorylation of EGFR, HER2 and HER3 (2,3). This in turn promotes activation of phosphatidylinositol 3-kinase (PI3K)-Akt and mitogen-activated protein kinase (MAPK) signaling, among other pathways, to promote cell proliferation and survival (4). Targeted agents against HER2 (e.g., lapatinib) have significantly improved

Corresponding Author: Dihua Yu, M.D., Ph.D., Department of Molecular and Cellular Oncology, MD Anderson Cancer Center, 1515 Holcombe Blvd, Houston, TX 77030 (dyu@mdanderson.org); Telephone: 713-792-3636; Fax: 713-792-4454.

Disclosure of Conflicts of Interest: The authors disclose no conflicts of interest.

clinical outcomes in patients having HER2-positive breast cancer (5-7). Yet resistance to the dual EGFR/HER2 kinase inhibitor lapatinib frequently occurs (8). Therapeutic options for such patients are limited; therefore identifying resistance mechanisms is crucial in order to develop effective treatments for these patients.

Activating mutations in the p110 α catalytic subunit of PI3K (*PIK3CA*) occur in 25% of HER2-positive breast cancers (9) and are believed to promote lapatinib (and trastuzumab) resistance through Akt activation (9-12). However some HER2-positive breast cancers and cell lines with PI3K mutations are lapatinib-sensitive (13-15). Here we show that such cancers may acquire resistance to lapatinib by further increasing PI3K signaling output through either upregulation of an existing PI3K p110 α mutant and/or a secondary p110 α mutation event. These findings could help differentiate HER2-positive, PI3K-mutant breast cancers that are lapatinib-sensitive from those that are lapatinib-resistant. The results suggest that targeting the PI3K mutation can be an effective strategy to overcome lapatinib resistance in HER2-positive and PI3K-mutant breast cancers.

Materials and Methods

Parental, lapatinib-resistant, and stable cell lines

BT474.m1 cells (BT474 hereafter) were described previously (16). UACC893 cells were from ATCC. Lapatinib-resistant (LapR) cells were derived by treating parental cells with 2.1 μ M lapatinib for >9 months (BT474) or increasing doses until reaching 2.1 μ M for a total of >5 months (UACC893). Cell lines were authenticated by the MD Anderson Characterized Cell Line Core Facility by short tandem repeat analysis (March 2013). HA-*PIK3CA* wild-type and H1047R (Addgene plasmids 12522, 12524) from Dr. Jean Zhao (17) were cloned into pLVX EF1a-IRES-ZsGreen (Clontech). HA-*PIK3CA* E542K was generated by site-directed mutagenesis. Following lentiviral infection cells were FACS-sorted to isolate ZsGreen-expressing cells.

Proliferation assays and siRNA transfection

For MTT proliferation assays, 3,000-10,000 cells per well were plated in 96-well plates, generally in triplicate for each treatment. siRNA (Sigma), if used, was transfected 1-2 days later at 10nM using PepMute (SignaGen). Medium was replaced the next day with drug- or vehicle-containing medium. When siRNA was not used, drug was added 1-2 days after plating. DMSO concentration was 0.1% and equal between treatments. 3-5 days after drug addition, 25-50 μ L/well of 5mg/mL MTT (Sigma) was added. 1-3 hours later, medium was replaced with 100 μ L DMSO and readings were performed after solubilization. 650 nm background optical densities (O.D.) were subtracted from 570 nm readings and normalized to vehicle. For crystal violet staining to visualize proliferation, 300,000 cells per well were plated in 6-well plates. 1-2 days later, siRNA transfection was performed and drugs were given in fresh medium one day after transfection. After 3-5 days of drug treatment, cells were fixed with 0.5% crystal violet, 6% glutaraldehyde for 30-60 minutes, followed by wash and imaging of wells. Lapatinib was withdrawn from LapR cells for 1 week before experiments.

Whole-exome sequencing

Genomic DNA (gDNA) was isolated using PureLink Genomic DNA Mini Kit (Life Technologies). Whole-exome sequencing performed by Otogenetics Corporation using NimbleGen V2 exome enrichment and Illumina HiSeq2000 sequencing was analyzed in DNA Nexus.

Reverse phase protein array (RPPA)

Cells were plated and processed per the MD Anderson RPPA Core Facility protocol, available online. Protein was isolated from cells, adjusted to 1-1.5mg/mL, boiled for 5 minutes after addition of 4x SDS sample buffer, stored at -80 °C, and later submitted to the MD Anderson RPPA Core Facility.

Western blot analysis

LapR cells underwent lapatinib withdrawal for 1 week before experiments and drugs were given in fresh medium. Protein was isolated from cells and 30µg protein per sample was analyzed by western blot as we have done previously (16). Antibodies were from GE Healthcare (secondary antibodies), Sigma (α-tubulin), or Cell Signaling. Films were scanned into Adobe Photoshop; quantification was performed in ImageJ. For siRNA knockdown efficiency, cells were harvested for western blot 3 days post-transfection.

qPCR

RNA isolated with TRIzol (Life Technologies) or RNazol (Molecular Research Center, Inc.) was reverse-transcribed using SuperScript III (Life Technologies). gDNA was isolated as with whole-exome sequencing. qPCR was done using SYBR FAST (Kapa Biosystems) or iQ SYBR Green or iTaq Universal SYBR Green Supermix (Bio-Rad). Primers recognizing *PIK3CA* E542K allele were: (forward) 5'-CAATGAATTAAGGGAAAATGACA-3'; (reverse) 5'-CTTTCTCCTGCTCAGTGATTCT-3'. These and other gDNA-specific primers used (wild-type *PIK3CA* and *LINE1*) were described previously (18,19). cDNA-specific primers were designed using standard techniques.

Cell cycle analysis

After indicated treatments, cells were harvested; fixed in cold 75% ethanol, 25% PBS 40 minutes on ice; washed; stained with 33µg/mL propidium iodide in PBS 20 minutes at 37 °C; and analyzed by flow cytometry. Doublets were gated out.

Xenograft studies

6-8-week-old female Swiss nude mice (MD Anderson Department of Experimental Radiation Oncology) received mammary fat pad (mfp) injections of 4.5 million BT474 LapR cells in 100µL 1:1 serum-free medium and growth factor-reduced Matrigel (BD Biosciences). Two tumors per mouse were injected on opposing middle mfps. Next day mice were treated with 31µg estrogen intraperitoneally (estradiol cypionate; Pfizer) to support tumor growth. 7 days later, tumors were measured and mice were randomized to treatment groups (15 mice each). The next day (day 1) treatments began as follows: lapatinib (48 mg/kg; GlaxoSmithKline and LC Laboratories), BYL719 (48mg/kg; Novartis), the combination of both, or vehicle by daily oral gavage. Lapatinib vehicle was 0.5% hydroxypropylmethylcellulose, 0.1% Tween-20; BYL719 vehicle was 0.5% methylcellulose. All mice received both vehicles. After apparent muzzle area dryness in BYL719 or combination-treated mice, each drug was reduced to 36mg/kg on day 6. Dryness was transient and dose from day 9 onward was 48mg/kg lapatinib and 36mg/kg BYL719. One week after treatment began, four tumors per treatment group were removed 5 hours after the daily drug treatment for western blot and immunohistochemistry. Estrogen was given as before on days 2, 12, 22, 33, and 44. Tumor volume was calculated as $(\text{length} \times \text{width}^2) / 2$ as measured by calipers on indicated days. Measurements were normalized to the day 0 mean (=100%) for each group. Animal weight was measured using a scale on indicated days starting on treatment day 6. Animals were sacrificed when cumulative tumor diameter became excessive.

Immunohistochemistry

Immunohistochemistry (IHC) was performed using Golden Bridge International kits as we have done previously (16). Antibodies were from Cell Signaling (p-Akt T308, #4056, 1:100; p-Erk1/2, #4370, 1:800).

Statistics

Student's t-test, ANOVA, or Mann-Whitney tests (as indicated in legends) were performed in Microsoft Excel or Graphpad Prism. $p < 0.05$ was considered statistically significant.

Results

PI3K p110 α activation is enhanced in lapatinib resistance models

To create models of lapatinib resistance, we treated the HER2-positive human breast cancer cell lines BT474 and UACC893 with lapatinib for longer than 5-9 months. The resulting acquired lapatinib-resistant cell lines (LapR) were highly resistant to lapatinib compared with parental cells (Fig. 1a).

To identify potential mechanism(s) of acquired lapatinib resistance, we analyzed levels of >170 proteins or phospho-proteins by reverse phase protein array (RPPA) (20) in parental versus LapR cells. We identified proteins/phospho-proteins increased at least 20% in either LapR cell line compared with parental counterparts, and seven were increased in both cell lines, one of which was PI3K p110 α (Fig. 1b). Consistent with our RPPA data, western blot analysis demonstrated that p110 α is increased about 2-fold in both LapR cell lines compared to parental cells (Fig. 1c). These data suggest that p110 α may be a key player in lapatinib resistance in both LapR models. Moreover, as both parental cell lines possess p110 α activating mutations (21), we hypothesized that increased expression of the mutant p110 α proteins may further enhance PI3K activation and contribute to lapatinib resistance in these LapR models.

To assess whether increased p110 α mutant proteins in LapR cells further enhanced PI3K activation, we detected phosphorylation of its downstream target Akt. Indeed, p-Akt T308 was reproducibly enhanced about 3-fold in BT474 LapR cells and about 2-fold in UACC893 LapR cells under lapatinib-treated conditions compared to parental cells (Fig. 1c). These data demonstrate that PI3K downstream signaling is enhanced in LapR cells compared to parental cells.

Notably, enhanced PI3K-Akt signaling and lapatinib resistance in LapR cells were not due to inability of lapatinib to inhibit HER2 (Fig. 1c), or HER3 (Supplementary Figures 1 and 2), the primary activator of PI3K in HER2-positive breast cancer (4,22,23). Thus enhanced Akt phosphorylation in LapR cells may result from enhanced p110 α protein. Notably, basal phosphorylation of HER2 (Fig. 1c) and HER3 (Supplementary Figure 1) were decreased in both LapR cell lines. This may be due to enhanced PI3K signaling in LapR cells, as it has been reported that PI3K inhibition increases HER2 and HER3 phosphorylation by promoting dimerization (24). Thus, PI3K activation may suppress HER2 and HER3 phosphorylation and activation. Additionally, LapR cells are less dependent on HER2, which may allow them to tolerate genetic losses or gains that lead to decreased HER2 activation, whereas the HER2-dependent parental cells would not tolerate such changes well.

Many mechanisms of PI3K activation exist, including mutational activation (12). We therefore tested whether, in addition to increased p110 α protein level, Akt activation in LapR cells may also result from additional PI3K mutations (or other genetic changes) in

LapR cell lines by performing whole-exome sequencing on parental and LapR cells. We identified a heterozygous E542K activating mutation of p110 α in BT474 LapR cells (36% of reads in the relevant position), which is not present in BT474 parental cells (Fig. 1d). This mutation is highly oncogenic (25,26) and one of three hotspot mutations in p110 α (27). Both BT474 parental and LapR cells possessed the K111N p110 α mutation previously reported in this cell line (21) (data not shown). As the E542K mutation is more oncogenic than K111N (25), these data suggest that an additional, stronger PI3K-activating mutation may promote lapatinib resistance in BT474 LapR cells. This may have occurred through selection of a rare sub-clone (28).

UACC893 parental and LapR cells both possessed the strongly oncogenic p110 α H1047R mutation (27) previously reported in this cell line (21) (data not shown). This may explain why UACC893 parental cells are more lapatinib-resistant than BT474 parental cells. (See Fig. 1a; the lapatinib IC₅₀ is ~50nM versus 200-400nM for BT474 and UACC893 parental cells, respectively.) In spite of this PI3K mutation, however, UACC893 parental cells were still lapatinib-sensitive at doses near 1 μ M, which is clinically achievable (7) (Fig. 1a). We did not identify any additional cancer-associated mutations in UACC893 LapR cells compared to UACC893 parental cells (data not shown). Thus non-genetic mechanisms, such as p110 α up-regulation (Fig. 1b, c), may promote lapatinib resistance in this case.

To summarize, UACC893 LapR cells have increased levels of p110 α H1047R, while BT474 LapR cells not only have increased mutant p110 α protein but also gained an additional p110 α E542K activating mutation. These data led us to propose that lapatinib resistance in these cell lines is a result of increased PI3K-Akt signaling through p110 α upregulation and/or mutation.

Knockdown of p110 α sensitizes lapatinib-resistant cells to lapatinib treatment

To test whether p110 α plays a critical role in lapatinib resistance of LapR cells, we knocked down p110 α using siRNA. We also knocked down PI3K p110 β , another class IA PI3K catalytic subunit (17), as a control for p110 α -specific function. Effective knockdown by each siRNA was confirmed by western blot (Fig. 2a). We compared the proliferation and lapatinib sensitivity of p110 α versus p110 β and control nonsilencing siRNA-treated LapR cells. We found that knockdown of p110 α , but not p110 β , significantly enhanced lapatinib sensitivity of BT474 LapR and UACC893 LapR cells by MTT assay (Fig. 2b) and crystal violet staining of cells (Supplementary Fig. 3). Thus PI3K p110 α promotes lapatinib resistance in these models. We note that p110 α knockdown by siRNA was less effective in UACC893 LapR than in BT474 LapR cells (Supplementary Fig. 4), which may explain why p110 α siRNA inhibited growth more effectively in BT474 LapR cells compared to UACC893 LapR cells (Fig. 2b). Although one p110 β siRNA (#2) induced a decrease in proliferation of BT474 LapR cells (Fig. 2b), this is likely due to off-target effects, as BT474 LapR cells treated with p110 β siRNA #2 had similar p110 β level as p110 β siRNA #1-treated cells (Fig. 2a), which showed no inhibition of proliferation. Moreover, p110 β siRNA #2 did not inhibit the proliferation of UACC893 LapR cells, indicating that p110 β siRNA #2's effects in BT474 LapR cells were due to off-target effects specific to BT474 LapR cells.

Overexpression of mutant p110 α is sufficient to confer lapatinib resistance

Previous studies demonstrated that p110 α E545K and H1047R mutations are sufficient to promote lapatinib resistance *in vitro* (10). However, the E542K mutation, found in many breast cancers and in BT474 LapR cells, was not analyzed. Therefore, we investigated whether p110 α E542K confers lapatinib resistance in BT474 parental (lapatinib-sensitive) cells. We stably infected BT474 parental cells with lentiviruses expressing HA-tagged p110 α wild-type (WT), E542K, or H1047R (as a positive control), and verified ectopic

expression at a similar level by western blot (Fig. 3a). Next, we measured these stable sub-lines for lapatinib sensitivity, and found that the E542K mutant, similar to H1047R, promoted lapatinib resistance in BT474 parental cells (Fig. 3b), whereas WT p110 α did not. WT, E542K, or H1047R p110 α transfected BT474 cells had significantly ($p < 0.01$) increased proliferation compared to vector controls (Supplementary Fig. 5). Notably, BT474 parental cells have low endogenous p110 α compared to the high ectopic p110 α levels in the stable sub-lines (Fig. 3a), likely due to the strong EF1a promoter used. Our data demonstrate that the E542K and H1047R mutations, but not WT p110 α , are sufficient to confer lapatinib resistance, at least at high expression levels. On the other hand, the endogenous level of the H1047R mutant in UACC893 parental cells does not render the cells fully lapatinib-resistant (Fig. 1a). These findings suggest a dose-dependent effect of mutant PI3K in lapatinib resistance. Indeed, we observed increased levels of mutant PI3K in both LapR cell lines.

PI3K protein level is increased in lapatinib-resistant cells through diverse mechanisms

p110 α protein was increased in both LapR cell lines (Fig. 1c). We tested whether this may be due to mRNA increase by qRT-PCR of *PIK3CA* (p110 α) mRNA. BT474 LapR cells possessed ~2-fold more *PIK3CA* mRNA than parental cells, while UACC893 LapR cells had no change (Fig. 4a). To test whether mRNA upregulation in BT474 LapR cells results from gene amplification, we performed qPCR of genomic DNA using primers recognizing genomic *PIK3CA*. BT474 LapR cells had 2-fold amplification of the *PIK3CA* gene compared with parental cells (Fig. 4b, left panel); UACC893 LapR cells had a slight decrease (Fig. 4b, right panel). This indicates that increased p110 α protein levels in different lapatinib-resistant cells can occur through divergent means: DNA amplification in one case and post-transcriptional mechanisms in another.

To test whether *PIK3CA* gene amplification in BT474 LapR cells involved the E542K allele, we performed qPCR of genomic DNA using E542K-specific primers. These primers preferentially amplify *PIK3CA* E542K due to stronger base pairing with the mutant nucleotide (18). We used BT483 breast cancer cells as a control for non-amplified *PIK3CA* E542K, as they harbor the E542K mutation (21). BT483 cells possessed similar genomic *PIK3CA* level to BT474 parental cells and a strong E542K-specific qPCR signal compared with parental BT474 cells (Fig. 4c), confirming that these cells harbored non-amplified E542K. Remarkably, qPCR signals of both total genomic *PIK3CA* and *PIK3CA* E542K in BT474 LapR cells were double that of BT483 cells (Fig. 4c), indicating that BT474 LapR cells possess amplification of the *PIK3CA* E542K allele. This raises an interesting possibility that the E542K mutant at a non-amplified level is insufficient to confer maximal lapatinib resistance in BT474 LapR cells and that amplification is necessary for a strong resistance phenotype. qPCR of gDNA from BT474 parental cell with E542K-specific primers did not yield amplification signals as did in BT474 LapR and BT483 cells until up to eight cycles later, consistent with lack of E542K mutation in BT474 parental cells (Fig. 4c, see double asterisk).

The p110 α -selective PI3K inhibitor BYL719 overcomes lapatinib resistance in vitro

Lapatinib resistance in our models was dependent on the p110 α , but not p110 β , PI3K subunit (Fig. 2a). Therefore, we hypothesized that a p110 α -selective PI3K inhibitor may overcome lapatinib resistance. BYL719 is a p110 α -selective PI3K inhibitor (29,30) showing encouraging results in clinical trials (31). Moreover, p110 α -specific inhibition may be better than pan-PI3K inhibition in p110 α -dependent malignancy due to decreased toxicity and thus better therapeutic index (32).

We treated LapR cells with BYL719 alone or combined with lapatinib and analyzed proliferation. We found that BYL719 effectively overcomes lapatinib resistance in a dose-

dependent manner (Fig. 5a). The combination inhibited proliferation synergistically in UACC893 LapR cells, but not in BT474 LapR cells (Supplementary Fig. 6). The combination also more effectively blocked Akt phosphorylation in LapR cells than either drug alone (Fig. 5b). Although BYL719 alone increased phosphorylation of HER2 and HER3, consistent with other PI3K inhibitors (24,33), lapatinib plus BYL719 effectively inhibited HER2 and HER3 phosphorylation (Fig. 5b, Supplementary Fig. 7).

To test whether lapatinib plus BYL719 functioned by inhibiting proliferation, inducing cell death, or both, we performed cell cycle analysis of drug-treated LapR cells. After 3 days of treatment we performed propidium iodide staining to analyze DNA content (Fig. 5c). In BT474 LapR cells, neither drug alone substantially altered the cell cycle profile (see Fig. 5d quantification; note that sub-G1 cells are excluded in this quantification). However, in combination-treated cells the sub-G1 population, indicative of dead or dying cell bodies with less DNA, was increased from less than 1.0% in vehicle-treated cells to 19.0% in combination-treated cells (see bars, Fig. 5c). Moreover, entrance into G2/M was inhibited in combination-treated cells, as indicated by the lower 4N DNA peak (22.1% of cells in DMSO versus 12.6% in combination; Fig. 5c, d), while the S phase population increased (5.2% in DMSO versus 17.2% in combination). The G1 phase was not affected by combination treatment. Together, these data suggest that the combination slowed S phase progression, leading to accumulation in S phase, and/or killed cells during G2/M. Thus the combination treatment both induces cell death and inhibits cell cycle progression in BT474 LapR cells.

In UACC893 LapR cells, the combination treatment increased the sub-G1 population from 11.7% in vehicle-treated cells to 41.2% and was superior to either drug alone (Fig. 5c). As with BT474 LapR cells, the combination increased the S phase population (from 8.2% in DMSO to 14.9% in combination; Fig. 5d). G1 phase cells decreased from 65.3% in DMSO-treated cells to 55.8% in combination treatment, suggesting that entrance into S phase was inhibited by the combination. There was no significant difference in G2/M population between DMSO and combination treatment (26.5% and 29.2%, respectively). Thus the combination treatment moderately inhibits G1 entry into S phase, and slows S phase progression to G2/M in UACC893 LapR cells. These cell cycle-inhibitory effects appear secondary, however, to the more dramatic cytotoxic effects of the combination in these cells.

BYL719 combined with lapatinib overcomes lapatinib resistance in vivo

We next performed pre-clinical testing to see whether lapatinib plus BYL719 might be a clinically applicable combination for overcoming lapatinib resistance. We established BT474 LapR xenografts in mammary fat pads (mfps) of nude mice with two xenografts per animal (third thoracic mfps). (UACC893 LapR cells were not efficiently tumorigenic in mice.) We then treated mice daily with lapatinib, BYL719, lapatinib plus BYL719, or vehicle control and measured tumor growth. Remarkably, tumor growth was completely inhibited by combination treatment, whereas tumor growth continued with either drug alone (Fig. 6a). Although lapatinib plus BYL719 effectively inhibited tumor growth, the residual tumors from this combination treatment maintained malignant morphology similar to other treatment groups (data not shown). Lapatinib plus BYL719 did not induce weight loss in mice (Supplementary Fig. 8). One out of 11 animals developed a skin rash and hunched posture and two others became slightly hunched under treatment (not shown); these three mice were reduced to intermittent half-dosing, which maintained tumor stasis and revealed that the toxicity was largely reversible. BYL719 alone did not induce significant weight loss when comparing the first measurement (day 6) to later measurements by one-way ANOVA. However, one-way ANOVA with post-test for linear trend indicated a statistically significant negative slope of weight over time in BYL719-treated mice ($p = 0.015$), consistent with loss of appetite in BYL719-treated cancer patients (31). Interestingly, this occurred in the BYL719-alone but not combination-treated mice.

To analyze target inhibition *in vivo* by each treatment, BT474 LapR xenografts were analyzed by western blot and IHC after one week of treatment (Fig. 6b, and Supplementary Fig. 9). Compared with vehicle-treated mice, lapatinib alone did not inhibit phosphorylation of HER family members, nor their downstream signals (Erk and Akt) in the LapR tumors, consistent with previous reports in BT474 xenografts (34). BYL719, however, effectively inhibited Akt phosphorylation, alone or combined with lapatinib (Fig. 6b; Supplementary Fig. 9). Similar to other PI3K inhibitors (24,33), BYL719 alone or combined with lapatinib induced phosphorylation of HER family members (Fig. 6b). Combination treatment demonstrated the most effective inhibition of Akt and Erk phosphorylation (Fig. 6b; Supplementary Fig. 9) even without inhibiting phosphorylation of their upstream activators EGFR, HER2, and HER3 (see Discussion). Diminished Erk phosphorylation upon combination treatment was unexpected, as PI3K inhibition was reported to enhance Erk activation through feedback mechanisms (24) (see Discussion). Together, our data demonstrate that BYL719 combined with lapatinib effectively overcomes acquired lapatinib resistance *in vivo*, potentially through inhibition of the Akt and Erk pathways.

Discussion

We have identified PI3K activation by p110 α protein upregulation and/or additional mutation as a mechanism of acquired lapatinib resistance. Ectopic expression of PI3K mutants has been shown to promote lapatinib resistance *in vitro* (10). However, this study is the first report that lapatinib resistance in PI3K-mutant, HER2-positive breast cancers can result from enhanced PI3K p110 α protein levels, as we have observed in two lapatinib resistance models. This suggests a possible threshold effect of mutant PI3K: low levels of mutant PI3K may not be sufficient to confer lapatinib resistance in breast cancer cells, while increased levels of mutant PI3K can make cancer cells resistant to lapatinib. As seen in our BT474 LapR cells, *PIK3CA* has been reported to be mutated and amplified simultaneously in breast tumors from some patients (35), which demonstrates that the expression levels of PI3K mutants varies between breast cancers. The up-regulation of p110 α in BT474 LapR cells was apparently due to gene amplification. However, in UACC893 LapR cells, p110 α up-regulation was not associated with increased gene copy number or mRNA. The p110 α protein upregulation could result from increased protein stability and/or translation in UACC893 LapR cells.

It will be important to determine whether the resistance mechanism identified can be detected in lapatinib-treated patients' tumor samples when tissues from lapatinib-treated patients become available. It should be noted that the approximately 2-fold increase in p110 α protein in BT474 LapR versus parental cell xenografts detected by western blot was not discernible by IHC (not shown), indicating that we need to develop better strategies to detect the differences in p110 α protein level in patient tissues.

Importantly, we have found that the lapatinib plus BYL719 combination can overcome acquired lapatinib resistance of breast cancer cells with simultaneous *PIK3CA* mutation and amplification. This suggests this combination may bring clinical benefit to patients. Another option may be to modify the current regimen of lapatinib treatment followed by trastuzumab/taxane therapy (13) by adding BYL719 to the lapatinib phase, especially, if patients tumors possess *PIK3CA* mutations.

Lapatinib failed to inhibit HER family member phosphorylation and their downstream effectors Akt and Erk in the BT474 LapR xenografts, which is consistent with previous findings in BT474 xenografts (34). The same study revealed effective tumor inhibition upon lapatinib treatment in spite of lack of HER2 phosphorylation inhibition. Similar to the findings from animal studies, lapatinib also fails to inhibit HER2 phosphorylation in a

significant proportion of lapatinib-treated breast cancer patients, yet this does not preclude clinical response (36). The reasons for this efficacy of lapatinib in spite of maintenance of receptor phosphorylation in these studies, and in our lapatinib plus BYL719 regimen, remains unclear and is very interesting.

The finding that lapatinib plus BYL719 inhibits Erk phosphorylation is unexpected, as others have shown that PI3K inhibition actually enhances Erk activation in BT474 cells (24). On the other hand, one group has reported that mutant PI3K induces Erk phosphorylation under serum-starved conditions (12). As our BT474 LapR xenograft model harbored a PI3K activating mutation, this may enhance Erk activation in this model. This may explain why both lapatinib and BYL719 are necessary to inhibit Erk phosphorylation, as the combination may allow more effective inhibition by inhibiting both HER2- and PI3K-induced Erk activation (Fig. 6B). Erk inhibition by the combination therapy could also be due to off-target effects of the drugs used. For example, lapatinib may have modest inhibitory effects on ATM, ATR, DNAPK, mTOR, JNK1, and CSNK1A1L kinases (37). Although lapatinib may inhibit EGFR/HER2 more effectively than these other kinases, the high level of amplification of HER2 in BT474 cells (10-fold or higher (38)) may make targeting these non-amplified targets easier than targeting HER2. Indeed, genetically amplified oncogenes are much harder to inhibit than non-amplified targets (39-41). Although the cause of lapatinib plus BYL719-induced Erk inhibition is unclear in our system, it is plausible that Erk inhibition contributes to the antitumor function of the combination treatment. We also observed that BYL719 induced phosphorylation of EGFR, HER2, and HER3 (as seen with other PI3K inhibitors (24,33)). Thus it will be interesting to see whether addition of trastuzumab to the combination regimen may further enhance therapeutic efficacy in future studies.

As the catalog of resistance mechanisms to various targeted therapies grows, it is encouraging to find some common patterns repeated in various resistance settings, such as PI3K- and Ras-induced resistance to RTK inhibitors (10,40,42-44), as well as activation of alternative RTKs (28,45-47). Indeed, with some targeted therapies, the majority of drug-resistant relapses can be classified by a known, identifiable (and often actionable) resistance mechanism (40,46,48,49). Therefore, it may soon be possible to define a “compendium” of resistance mechanisms for a given drug, along with a therapeutic means to overcome each one. This is a highly desirable goal that may fulfill the potential of targeted therapy to significantly reduce cancer mortality in this decade.

Supplementary Material

Refer to Web version on PubMed Central for supplementary material.

Acknowledgments

We thank Novartis for BYL719 and GlaxoSmithKline for providing lapatinib. Thanks to Dr. Dajun Yang for BT474.m1 cells, Drs. Siyuan Zhang and Ozgur Sahin for helpful discussions, Frank Lowery and Dr. Qingling Zhang for technical assistance, and Dr. Jean Zhao for plasmids deposited with Addgene.

Financial Support: This research was supported by F31 NIH/NCI award F31CA165819 (S.W. Brady), NIH grants P30-CA 16672 (MD Anderson Cancer Center), PO1-CA099031 project 4 (D. Yu), RO1-CA112567-06 (D. Yu), Susan G. Komen Breast Cancer Foundation Promise Grant KG091020 (D. Yu), and Cancer Prevention Research Institute of Texas Grant RP100726 (D. Yu). D. Yu is the Hubert L. & Olive Stringer Distinguished Chair in Basic Science at MD Anderson Cancer Center.

References

1. Slamon D, Godolphin W, Jones L, Holt J, Wong S, Keith D, et al. Studies of the HER-2/neu proto-oncogene in human breast and ovarian cancer. *Science*. 1989; 244:707–12. [PubMed: 2470152]
2. Junttila TT, Akita RW, Parsons K, Fields C, Lewis Phillips GD, Friedman LS, et al. Ligand-independent HER2/HER3/PI3K complex is disrupted by trastuzumab and is effectively inhibited by the PI3K inhibitor GDC-0941. *Cancer Cell*. 2009; 15:429–40. [PubMed: 19411071]
3. Stern DF. ERBB3/HER3 and ERBB2/HER2 duet in mammary development and breast cancer. *J. Mammary Gland Biol. Neoplasia*. 2008; 13:215–23. [PubMed: 18454306]
4. Hynes NE, Lane H a. ERBB receptors and cancer: the complexity of targeted inhibitors. *Nat. Rev. Cancer*. 2005; 5:341–54. [PubMed: 15864276]
5. Vogel CL. Efficacy and Safety of Trastuzumab as a Single Agent in First-Line Treatment of HER2-Overexpressing Metastatic Breast Cancer. *J. Clin. Oncol*. 2002; 20:719–26. [PubMed: 11821453]
6. Geyer CE, Forster J, Lindquist D, Chan S, Romieu CG, Pienkowski T, et al. Lapatinib plus capecitabine for HER2-positive advanced breast cancer. *N. Engl. J. Med*. 2006; 355:2733–43. [PubMed: 17192538]
7. Burris HA, Hurwitz HI, Dees EC, Dowlati A, Blackwell KL, O'Neil B, et al. Phase I safety, pharmacokinetics, and clinical activity study of lapatinib (GW572016), a reversible dual inhibitor of epidermal growth factor receptor tyrosine kinases, in heavily pretreated patients with metastatic carcinomas. *J. Clin. Oncol*. 2005; 23:5305–13. [PubMed: 15955900]
8. Garrett JT, Arteaga CL. Resistance to HER2-directed antibodies and tyrosine kinase inhibitors: Mechanisms and clinical implications. *Cancer Biol. Ther*. 2011; 11:793–800. [PubMed: 21307659]
9. Berns K, Horlings HM, Hennessy BT, Madiredjo M, Hijmans EM, Beelen K, et al. A functional genetic approach identifies the PI3K pathway as a major determinant of trastuzumab resistance in breast cancer. *Cancer Cell*. 2007; 12:395–402. [PubMed: 17936563]
10. Eichhorn PJA, Gili M, Scaltriti M, Serra V, Guzman M, Nijkamp W, et al. Phosphatidylinositol 3-kinase hyperactivation results in lapatinib resistance that is reversed by the mTOR/phosphatidylinositol 3-kinase inhibitor NVP-BE235. *Cancer Res*. 2008; 68:9221–30. [PubMed: 19010894]
11. Wang L, Zhang Q, Zhang J, Sun S, Guo H, Jia Z, et al. PI3K pathway activation results in low efficacy of both trastuzumab and lapatinib. *BMC Cancer*. 2011; 11:248. [PubMed: 21676217]
12. Isakoff SJ, Engelman JA, Irie HY, Luo J, Brachmann SM, Pearline RV, et al. Breast cancer-associated PIK3CA mutations are oncogenic in mammary epithelial cells. *Cancer Res*. 2005; 65:10992–1000. [PubMed: 16322248]
13. Dave B, Migliaccio I, Gutierrez MC, Wu M-F, Chamness GC, Wong H, et al. Loss of phosphatase and tensin homolog or phosphoinositol-3 kinase activation and response to trastuzumab or lapatinib in human epidermal growth factor receptor 2-overexpressing locally advanced breast cancers. *J. Clin. Oncol*. 2011; 29:166–73. [PubMed: 21135276]
14. O'Brien NA, Browne BC, Chow L, Wang Y, Ginther C, Arboleda J, et al. Activated phosphoinositide 3-kinase/AKT signaling confers resistance to trastuzumab but not lapatinib. *Mol. Cancer Ther*. 2010; 9:1489–502. [PubMed: 20501798]
15. Konecny GE, Pegram MD, Venkatesan N, Finn R, Yang G, Rahmeh M, et al. Activity of the dual kinase inhibitor lapatinib (GW572016) against HER-2-overexpressing and trastuzumab-treated breast cancer cells. *Cancer Res*. 2006; 66:1630–9. [PubMed: 16452222]
16. Zhang S, Huang W-C, Li P, Guo H, Poh S-B, Brady SW, et al. Combating trastuzumab resistance by targeting SRC, a common node downstream of multiple resistance pathways. *Nat. Med*. 2011; 17:461–9. [PubMed: 21399647]
17. Zhao JJ, Liu Z, Wang L, Shin E, Loda MF, Roberts TM. The oncogenic properties of mutant p110alpha and p110beta phosphatidylinositol 3-kinases in human mammary epithelial cells. *Proc. Natl. Acad. Sci. U. S. A*. 2005; 102:18443–8. [PubMed: 16339315]
18. Board RE, Thelwell NJ, Ravetto PF, Little S, Ranson M, Dive C, et al. Multiplexed assays for detection of mutations in PIK3CA. *Clin. Chem*. 2008; 54:757–60. [PubMed: 18375489]

19. Chiang W-F, Liu S-Y, Yen C-Y, Lin C-N, Chen Y-C, Lin S-C, et al. Association of epidermal growth factor receptor (EGFR) gene copy number amplification with neck lymph node metastasis in areca-associated oral carcinomas. *Oral Oncol.* 2008; 44:270–6. [PubMed: 17468034]
20. Tibes R, Qiu Y, Lu Y, Hennessy B, Andreeff M, Mills GB, et al. Reverse phase protein array: validation of a novel proteomic technology and utility for analysis of primary leukemia specimens and hematopoietic stem cells. *Mol. Cancer Ther.* 2006; 5:2512–21. [PubMed: 17041095]
21. Hollestelle A, Elstrodt F, Nagel JHA, Kallemeijn WW, Schutte M. Phosphatidylinositol-3-OH kinase or RAS pathway mutations in human breast cancer cell lines. *Mol. Cancer Res.* 2007; 5:195–201. [PubMed: 17314276]
22. Garrett JT, Olivares MG, Rinehart C, Granja-Ingram ND, Sánchez V, Chakrabarty A, et al. Transcriptional and posttranslational up-regulation of HER3 (ErbB3) compensates for inhibition of the HER2 tyrosine kinase. *Proc. Natl. Acad. Sci. U. S. A.* 2011; 108:5021–6. [PubMed: 21385943]
23. Lee-Hoeflich ST, Crocker L, Yao E, Pham T, Munroe X, Hoeflich KP, et al. A central role for HER3 in HER2-amplified breast cancer: implications for targeted therapy. *Cancer Res.* 2008; 68:5878–87. [PubMed: 18632642]
24. Serra V, Scaltriti M, Prudkin L, Eichhorn PJA, Ibrahim YH, Chandarlapaty S, et al. PI3K inhibition results in enhanced HER signaling and acquired ERK dependency in HER2-overexpressing breast cancer. *Oncogene.* 2011; 30:2547–57. [PubMed: 21278786]
25. Gymnopoulos M, Elsliger M-A, Vogt PK. Rare cancer-specific mutations in PIK3CA show gain of function. *Proc. Natl. Acad. Sci. U. S. A.* 2007; 104:5569–74. [PubMed: 17376864]
26. Zhao L, Vogt PK. Helical domain and kinase domain mutations in p110alpha of phosphatidylinositol 3-kinase induce gain of function by different mechanisms. *Proc. Natl. Acad. Sci. U. S. A.* 2008; 105:2652–7. [PubMed: 18268322]
27. Vogt PK, Kang S, Elsliger M-A, Gymnopoulos M. Cancer-specific mutations in phosphatidylinositol 3-kinase. *Trends Biochem. Sci.* 2007; 32:342–9. [PubMed: 17561399]
28. Turke AB, Zejnullahu K, Wu Y-L, Song Y, Dias-Santagata D, Lifshits E, et al. Preexistence and clonal selection of MET amplification in EGFR mutant NSCLC. *Cancer Cell.* 2010; 17:77–88. [PubMed: 20129249]
29. Furet P, Guagnano V, Fairhurst RA, Imbach-Weese P, Bruce I, Knapp M, et al. Discovery of NVP-BYL719 a potent and selective phosphatidylinositol-3 kinase alpha inhibitor selected for clinical evaluation. *Bioorg. Med. Chem. Lett.* 2013; 23:3741–8. [PubMed: 23726034]
30. Young CD, Pfefferle AD, Owens P, Kuba MG, Rexer BN, Balko JM, et al. Conditional loss of ErbB3 delays mammary gland hyperplasia induced by mutant PIK3CA without affecting mammary tumor latency, gene expression or signaling. *Cancer Res.* 2013; 73:4075–4085. [PubMed: 23633485]
31. Juric D, Rodon J, Gonzalez-Angulo A. BYL719, a next generation PI3K alpha specific inhibitor: Preliminary safety, PK, and efficacy results from the first-in-human study. *Cancer Research.* 2012; 72(8 supplement)
32. Engelman JA. Targeting PI3K signalling in cancer: opportunities, challenges and limitations. *Nat. Rev. Cancer.* 2009; 9:550–62. [PubMed: 19629070]
33. Chakrabarty A, Sánchez V, Kuba MG, Rinehart C, Arteaga CL. Feedback upregulation of HER3 (ErbB3) expression and activity attenuates antitumor effect of PI3K inhibitors. *Proc. Natl. Acad. Sci. U. S. A.* 2012; 109:2718–23. [PubMed: 21368164]
34. Rimawi MF, Wiechmann LS, Wang Y-C, Huang C, Migliaccio I, Wu M-F, et al. Reduced dose and intermittent treatment with lapatinib and trastuzumab for potent blockade of the HER pathway in HER2/neu-overexpressing breast tumor xenografts. *Clin. Cancer Res.* 2011; 17:1351–61. [PubMed: 21138857]
35. Kadota M, Sato M, Duncan B, Ooshima A, Yang HH, Diaz-Meyer N, et al. Identification of novel gene amplifications in breast cancer and coexistence of gene amplification with an activating mutation of PIK3CA. *Cancer Res.* 2009; 69:7357–65. [PubMed: 19706770]
36. Spector NL, Xia W, Burris H, Hurwitz H, Dees EC, Dowlati A, et al. Study of the biologic effects of lapatinib, a reversible inhibitor of ErbB1 and ErbB2 tyrosine kinases, on tumor growth and survival pathways in patients with advanced malignancies. *J. Clin. Oncol.* 2005; 23:2502–12. [PubMed: 15684311]

37. Bantscheff M, Eberhard D, Abraham Y, Bastuck S, Boesche M, Hobson S, et al. Quantitative chemical proteomics reveals mechanisms of action of clinical ABL kinase inhibitors. *Nat. Biotechnol.* 2007; 25:1035–44. [PubMed: 17721511]
38. Kallioniemi O. ERBB2 Amplification in Breast Cancer Analyzed by Fluorescence in situ Hybridization. *Proc. Natl. Acad. Sci.* 1992; 89:5321–5. [PubMed: 1351679]
39. Shi H, Moriceau G, Kong X, Lee M-K, Lee H, Koya RC, et al. Melanoma whole-exome sequencing identifies (V600E)B-RAF amplification-mediated acquired B-RAF inhibitor resistance. *Nat. Commun.* 2012; 3:724. [PubMed: 22395615]
40. Sequist LV, Waltman BA, Dias-Santagata D, Digumarthy S, Turke AB, Fidias P, et al. Genotypic and histological evolution of lung cancers acquiring resistance to EGFR inhibitors. *Sci. Transl. Med.* 2011; 3:75ra26.
41. Katayama R, Shaw AT, Khan TM, Mino-Kenudson M, Solomon BJ, Halmos B, et al. Mechanisms of acquired crizotinib resistance in ALK-rearranged lung Cancers. *Sci. Transl. Med.* 2012; 4:120ra17.
42. Han S-W, Kim T-Y, Jeon YK, Hwang PG, Im S-A, Lee K-H, et al. Optimization of patient selection for gefitinib in non-small cell lung cancer by combined analysis of epidermal growth factor receptor mutation, K-ras mutation, and Akt phosphorylation. *Clin. Cancer Res.* 2006; 12:2538–44. [PubMed: 16638863]
43. Diaz LA, Williams RT, Wu J, Kinde I, Hecht JR, Berlin J, et al. The molecular evolution of acquired resistance to targeted EGFR blockade in colorectal cancers. *Nature.* 2012; 486:537–40. [PubMed: 22722843]
44. Nagata Y, Lan K-H, Zhou X, Tan M, Esteva FJ, Sahin AA, et al. PTEN activation contributes to tumor inhibition by trastuzumab, and loss of PTEN predicts trastuzumab resistance in patients. *Cancer Cell.* 2004; 6:117–27. [PubMed: 15324695]
45. Liu L, Greger J, Shi H, Liu Y, Greshock J, Annan R, et al. Novel mechanism of lapatinib resistance in HER2-positive breast tumor cells: activation of AXL. *Cancer Res.* 2009; 69:6871–8. [PubMed: 19671800]
46. Zhang Z, Lee JC, Lin L, Olivas V, Au V, LaFramboise T, et al. Activation of the AXL kinase causes resistance to EGFR-targeted therapy in lung cancer. *Nat. Genet.* 2012; 44:852–60. [PubMed: 22751098]
47. Nazarian R, Shi H, Wang Q, Kong X, Koya RC, Lee H, et al. Melanomas acquire resistance to B-RAF(V600E) inhibition by RTK or N-RAS upregulation. *Nature.* 2010; 468:973–7. [PubMed: 21107323]
48. Ercan D, Xu C, Yanagita M, Monast CS, Pratilas CA, Montero J, et al. Reactivation of ERK signaling causes resistance to EGFR kinase inhibitors. *Cancer Discov.* 2012; 2:934–47. [PubMed: 22961667]
49. Takezawa K, Pirazzoli V, Arcila ME, Nebhan CA, Song X, de Stanchina E, et al. HER2 amplification: a potential mechanism of acquired resistance to EGFR inhibition in EGFR-mutant lung cancers that lack the second-site EGFR T790M mutation. *Cancer Discov.* 2012; 2:922–33. [PubMed: 22956644]

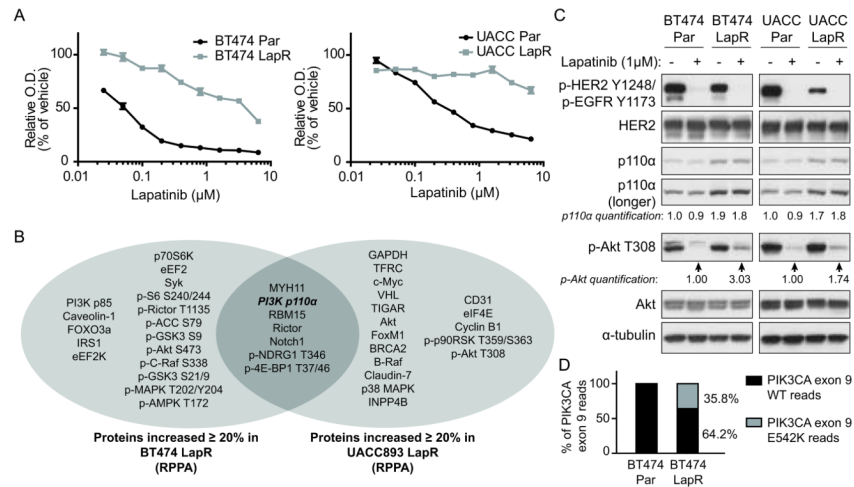


Figure 1. Lapatinib-resistant cells feature enhanced PI3K p110 α activation. (a) BT474 and UACC893 parental (Par) and LapR cells were treated for 4 days (BT474) or 3 days (UACC893) as shown followed by MTT assay. (O.D., optical density, is an indicator of cell number.) Results are representative of two independent experiments. Error bars, s.e.m. (b) Reverse phase protein array (RPPA) analysis was performed on BT474 and UACC893 parental and LapR cells. Proteins increased $\geq 20\%$ in LapR versus parental cells are shown. (c) Cells were treated 4.5 hours (BT474) or 4 hours (UACC893) with DMSO or $1\mu\text{M}$ lapatinib, followed by western blot. (d) Whole-exome sequencing was performed on genomic DNA and percent of WT and mutant reads at position corresponding to codon 542 in p110 α (*PIK3CA* gene) were compared in BT474 parental versus LapR cells.

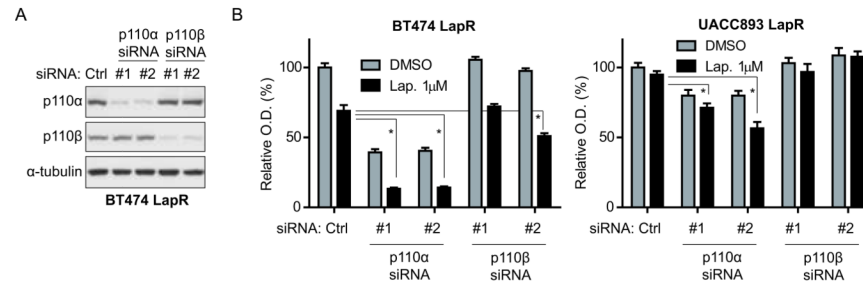


Figure 2.

Knockdown of p110 α enhances lapatinib sensitivity of lapatinib-resistant cells. (a) BT474 LapR cells were transfected with siRNA followed by western blot 3 days later. (b) BT474 and UACC893 LapR cells were transfected with p110 α or p110 β siRNA and given DMSO or 1 μ M lapatinib the next day. MTT assay was performed 3 days later. Error bars, s.e.m. (*p < 0.01 by one-way ANOVA of lapatinib-treated groups.)

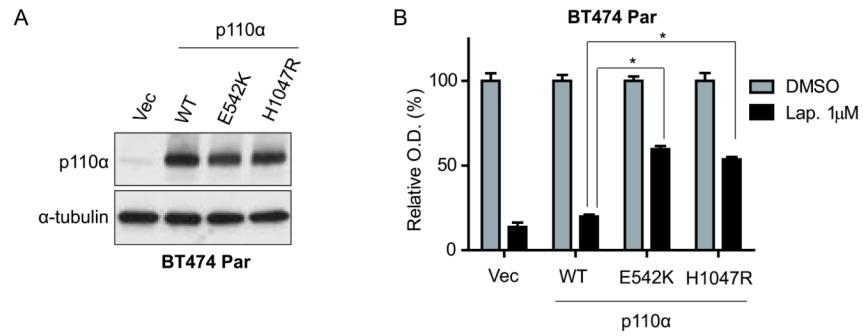


Figure 3. p110α hotspot mutations promote lapatinib resistance. (a) BT474 parental (Par) cells were infected with wild-type (WT) HA-tagged p110α, indicated mutants, or vector (Vec) followed by western blot. (b) Cells from (a) were treated 4 days as shown, followed by MTT assay. O.D. readings were normalized to each transductant's DMSO-treated reading (=100%). Error bars, s.e.m. (* $p < 0.001$ by one-way ANOVA of lapatinib-treated groups.)

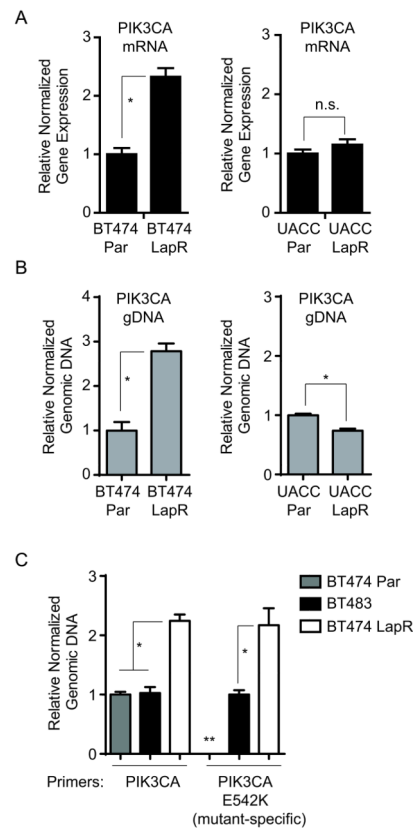


Figure 4.

p110 α is increased through diverse mechanisms in lapatinib-resistant cells. (a) qRT-PCR was performed using primers for *PIK3CA* and *ACTB* (β -actin) for normalization. (b) qPCR of genomic DNA was performed using primers recognizing genomic *PIK3CA*. *LINE1* was used for normalization. (c) qPCR of genomic DNA was performed as in (b) with allele-specific primers to *PIK3CA* E542K. BT474 parental (Par) gDNA was defined as 1.0 for total *PIK3CA* primers and BT483 gDNA was defined as 1.0 for E542K-specific primers. Results are the average from two independent experiments. (Error bars, s.e.m. * $p < 0.01$ by student's t-test (panels (a),(b), and right section of (c)) or one-way ANOVA (panel (c), left section); n.s., not significant. The double asterisk (**)) indicates that the data were not reliably measured for qPCR of BT474 Par gDNA with *PIK3CA* E542K-specific primers.)

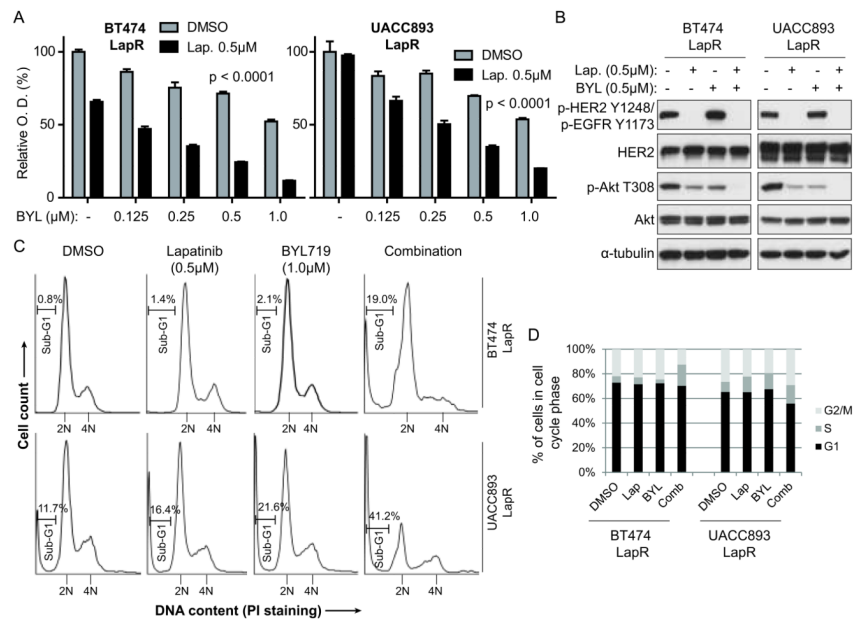


Figure 5. The p110 α -specific PI3K inhibitor BYL719 overcomes lapatinib resistance in vitro. (a) LapR cells were treated as shown for 4 days followed by MTT assay. Error bars, s.e.m. BYL and Lap. indicate BYL719 and lapatinib, respectively. (b) LapR cells were treated as shown for 3 hours followed by western blot. (c) LapR cells were treated as shown for 3 days followed by propidium iodide staining and flow cytometric cell cycle analysis. (d) Quantification of cell cycle analysis in (c). Comb indicates lapatinib plus BYL719 combination. Sub-G1 and super-G2 cells were excluded. ($p < 0.0001$ in panel (a) is by one-way ANOVA of lapatinib-treated groups with post-test for linear trend to analyze dose-dependent effect.)

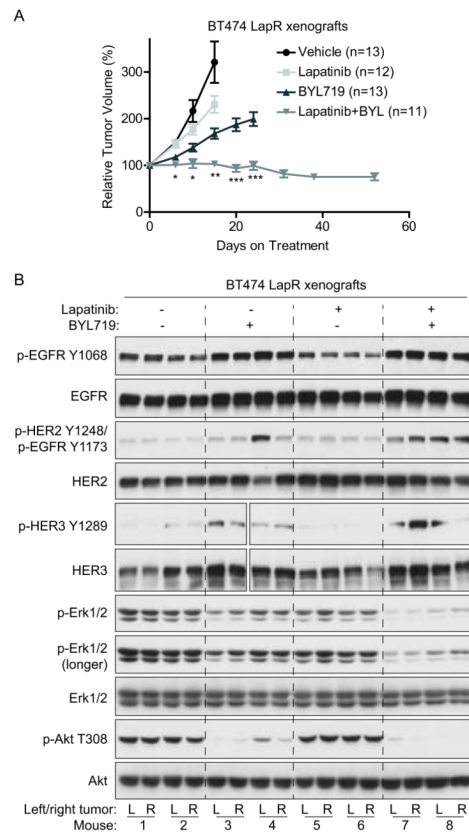


Figure 6.

BYL719 combined with lapatinib overcomes lapatinib resistance in BT474 LapR xenografts. (a) Mice with BT474 LapR xenografts were treated with 48 mg/kg lapatinib, 36 mg/kg BYL719, both drugs, or vehicle by oral gavage daily (see Materials and Methods). Tumors were measured on indicated days and volumes were normalized to day 0. Mice were sacrificed once tumor burden exceeded institutional euthanasia requirements. Error bars, s.e.m. (b) Xenografts from (a) were harvested for western blot on treatment day 7, ~5 hours after daily drug treatment. Four tumors (two mice) per group were analyzed. L, left mfp tumor; R, right. Gaps in HER3 blots result from accidental skipping of one lane; side-by-side HER3 images are from the same blot. p-Erk1/2 antibody recognizes p-Erk1 (T202/Y204 or T202 only; upper band) and p-Erk2 (T185/Y187 or T185 only; lower band). (* $p < 0.05$ by Kruskal-Wallis one-way ANOVA of lapatinib+BYL719 versus vehicle or lapatinib alone; ** $p < 0.05$ for lapatinib+BYL719 versus all groups; *** $p < 0.0001$ by Mann-Whitney test comparing lapatinib+BYL719 versus BYL719 alone.)